

# Morphological and Crystallographic Characterizations of the Ca-Mg-Zn Intermetallics Appearing in Ternary Diffusion Couples

Yi-Nan Zhang<sup>1, a</sup>, Dmytro Kevorkov<sup>1, b</sup>, Florent Bridier<sup>2, c</sup>  
and Mamoun Medraj<sup>1, d</sup>

<sup>1</sup>Department of Mechanical Engineering, Concordia University,  
1455 de Maisonneuve Blvd. W., Montreal, Quebec, H3G 1M8, Canada

<sup>2</sup>Department of Mechanical Engineering, Ecole de Technologie Supérieure, 1100 rue Notre-Dame  
Ouest, Montreal, Quebec, H3C 1K3, Canada

Email: <sup>a</sup>z\_yinan@encs.concordia.ca, <sup>b</sup>kevorkov@encs.concordia.ca,  
<sup>c</sup>florent.bridier@etsmtl.ca, <sup>d</sup>mmedraj@encs.concordia.ca

**Keywords:** Ca-Mg-Zn; phase diagrams; diffusion couples; X-ray diffraction; electron microprobe.

## Abstract

In the present research, seven multi-phase diffusion couples, with terminal alloys having different microstructural features, were prepared and annealed for 4 weeks at 335°C. The phase relations and change of morphological characteristics of each phase were studied along the diffusion zone by means of scanning electron microscopy/energy dispersive X-ray spectroscopy and quantitative electron probe microanalysis. Depending on the different terminal compositions of the diffusion couples, the morphological evolution in the diffusion zone can be: tooth-like, matrix phase with isolated and/or dendritic precipitates. Electron back-scattered diffraction analysis was carried out to investigate the crystal orientation of the ternary compounds and the crystal orientation relations at the interface of the diffusion zones.

## Introduction

Mg-based alloys have attracted considerable attention as the lightest structural alloys for the aerospace and automotive applications. The addition of Ca and Zn elements in alloys enhances the strength, castability, creep and corrosion resistance, fracture toughness and age hardening response [1-3]. Recently biocompatible glassy alloys were discovered in the Ca-Mg-Zn ternary system for the development of biodegradable implants [1-6]. Since the Ca-Mg-Zn system is promising as a next-generation material in both transportation and biomedical applications, understanding the equilibrium and the existence of the ternary intermetallics in this system are significant. Many researchers have studied the Ca<sub>2</sub>Mg<sub>6</sub>Zn<sub>3</sub> compound, but their results are contradictory [7-12]. More recently, the homogeneity range and crystal structure of this Mg-rich solid solution were determined using SEM, EPMA/WDS, TEM and X-ray diffraction by our group [13]. This compound has the Ca<sub>3</sub>Mg<sub>x</sub>Zn<sub>15-x</sub> (4.6 ≤ x ≤ 12) (IM1) formula at 335°C and it has a hexagonal structure with space group P63/mmc (194) and Sc<sub>3</sub>Ni<sub>11</sub>Si<sub>4</sub> prototype. The solubility ranges and X-ray diffraction (XRD) pattern of another ternary compound Ca<sub>2</sub>Mg<sub>5</sub>Zn<sub>13</sub> (IM3) were reported by Clark [8,14], but he did not provide any crystallographic information for it. The metallic glass and the region of biodegradability and biocompatibility were reported by Zberg et al. [4] and Ma and Xu [6].

The present study employs the high throughput diffusion couple technique, a valuable experimental approach for mapping the phase diagram of ternary systems [15-17]. In the diffusion couples or diffusion multiples, there are no problems associated with melting or powder contamination since all the phases are formed by diffusion mechanisms of the bulk constituents at the temperature of interest [18]. Within the diffusion layers the equilibrium phases occur, whereas local equilibrium takes place at the interface [18]. However, the diffusion couple approach is not infallible, and when it is used to determine phase diagrams, one should always consider the possibility of missing some of the phases [16,18]. This possibility may occur since the nucleation of these phases can be so slow that the formed diffusion layers are too thin to be detected by EPMA. This can result in inaccuracies

in estimating tie-line compositions for these phases because of errors in extrapolating inadequate number of data points. To solve this problem and to ensure the consistency of the analysis, other diffusion couples with different terminal compositions were used in the present work to compare and determine the phase equilibria.

### Experimental procedures

In order to study the Ca-Mg-Zn ternary system, seven diffusion couples were prepared to map the entire Ca-Mg-Zn composition range at 335°C based on the preliminary thermodynamic model of Wasiur-Rahman and Medraj [19]. The starting materials were Mg (purity 99.98%), Zn (99.99%) ingots and Ca (99%) supplied by Alfa Aesar. The key alloys were prepared in an arc-melting furnace with water-cooled copper crucible in an argon atmosphere using a non-consumable tungsten electrode. Samples were remelted five times to ensure their homogeneity. To prepare solid-state diffusion couples, the contacting surfaces are grinded down to 1200 grit SiC paper and polished using 1µm water-based diamond suspension and 99% pure ethanol as a lubricant. Two terminal members are carefully pressed together and clamped using a steel ring, placed in a Ta container, and sealed in a quartz tube filled with argon. The encapsulated samples are then annealed at 335°C for 4 weeks followed by quenching in water. Two solid-state diffusion couples are presented in this paper, as shown in Fig. 1.

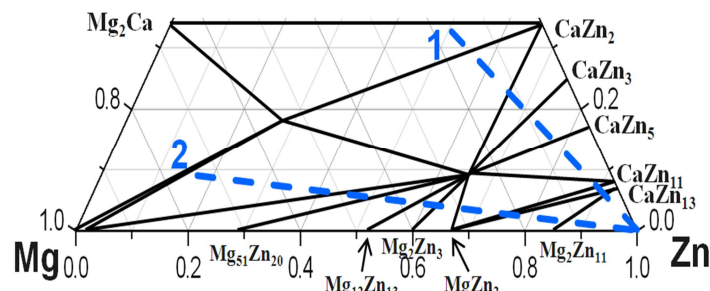


Fig. 1. Terminal compositions of the diffusion couples superimposed on the calculated isothermal section of the Ca-Mg-Zn system at 335°C on the basis of the thermodynamic model in [19].

The microstructure, layer thickness, phase composition, and homogeneity ranges were analyzed using quantitative electron probe microanalysis (EPMA) (JEOL-JXA-8900) with a 2µm probe diameter, 15kV accelerating voltage, 20nA probe current. Phi-Rho-Z (PRZ) matrix corrections (modified ZAF) are applied during the analysis. The error of the EPMA measurements is estimated to be about ±2 at.%. This value is obtained using statistical analysis of the compositions of selected phases from several samples. XRD is used for phase analysis and determination of the solubility limits in the key alloys. The XRD patterns are obtained using PANalytical X'pert Pro powder X-ray diffractometer with a CuKα radiation at 45kV and 40mA. The XRD spectrum is acquired from 20 to 120° 2θ with a 0.02° step size. X-ray diffraction study of the samples is carried out using X'Pert HighScore Plus Rietveld analysis software in combination with Pearson's crystal database [20]. To improve the surface condition for electron back-scattered diffraction (EBSD) measurements, the samples were first subjected to a standard mechanical metallographic procedure, then cleaned with plasma, ion milled, and again cleaned with plasma. EBSD analysis was performed using a Hitachi SU-70 Schottky-scanning electron microscopy (SEM) equipped with a Nordlys F+ camera and Oxford HKL Channel 5 software. Typical operation parameters were a 20 kV accelerating voltage and a 13 nA beam current. Surface topographic features were observed in secondary electron images (SEIs). Phases were identified by comparing experimental Kikuchi diffraction patterns with patterns computer-generated from parameters of the known structure.

## Results and discussion

Back-scattered electron (BSE) images of the solid-solid DC1 with gradually increased magnification of the area of interest are illustrated in Fig. 2. During heat treatment, extensive interdiffusion among Ca, Mg and Zn took place allowing various equilibrium phases to form. Based on the compositional information obtained by EPMA analysis, ternary and binary intermetallic compounds and the solid solubility of the binary compounds extending in the ternary system were identified. Using the local equilibrium at the interfaces formed between the phases, the sequence of the phases along the diffusion path is:  $\text{Zn} \rightarrow \text{CaZn}_{13} \rightarrow (\text{CaZn}_{11}) \rightarrow \text{CaZn}_5 + (\text{CaZn}_{11}) \rightarrow \text{CaZn}_3 + \text{IM2} \rightarrow \text{CaZn}_2 + \text{IM2} \rightarrow \text{CaZn}_2 + (\text{IM1}) \rightarrow (\text{Mg}_2\text{Ca}) + \text{CaZn}_2$ . Two ternary intermetallic compounds were detected in this diffusion couple by EPMA spot analysis: ternary intermetallic 1 (IM1) with composition 16.7 at.% Ca, 26.0 at.% Mg, and 57.3 at.% Zn and stoichiometric intermetallic 2 (IM2) with composition 14.4 at.% Ca, 15.8 at.% Mg, and 69.8 at.% Zn. The morphological feature of the diffusion zone evolved in a very irregular fashion in this diffusion couple forming a tooth-like structure shown in Fig. 2(b).

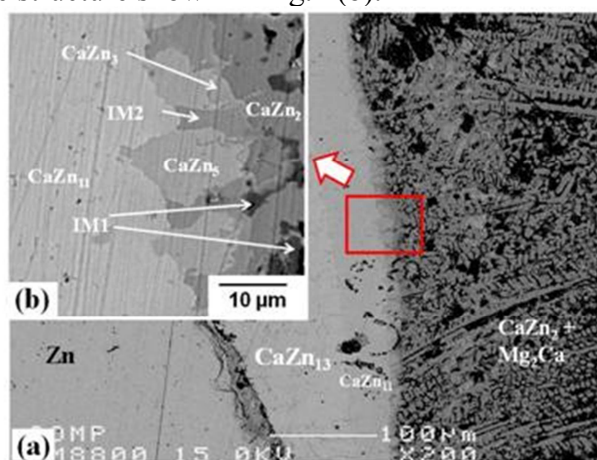


Fig. 2. BSE of the solid-state DC1 annealed at 335°C for 4 weeks.

The BSE image of the solid-solid DC2 (Fig. 3(a)) shows the formation of five different intermetallic compounds. On the basis of the compositional information obtained from quantitative EPMA, Electron backscattered diffraction (EBSD) analysis was performed to verify the crystallographic information. Two ternary intermetallic compounds IM1 (hP36) [15] and IM3 (hP92) were confirmed by both EPMA and EBSD. Determination of the crystal structure by EBSD is extremely useful for analyzing this system. Since these phases have similar compositions, EPMA data alone is not enough to identify them. A detailed description of the crystal structure of the IM1 ternary compound was reported in our previous paper [15]. The composition, homogeneity range and crystal structure of IM3 ternary phase have been identified by XRD, EPMA and TEM and the details will be published elsewhere. Fig 3(b) shows the indexed EBSD patterns of IM1, IM3 and  $\text{MgZn}_2$  phases. Analysis of the diffusion reaction zone reveals that the sequence of phases along the diffusion path is:  $(\text{IM1}) + (\text{Mg}) \rightarrow (\text{IM3}) + (\text{MgZn}_2) \rightarrow (\text{CaZn}_{13}) + (\text{MgZn}_2) \rightarrow (\text{CaZn}_{13}) + \text{Mg}_2\text{Zn}_{11} \rightarrow \text{Mg}_2\text{Zn}_{11} \rightarrow \text{Zn}$ . The following three-phase triangulations were identified from Fig. 3(a): (IM3),  $(\text{CaZn}_{13})$  and  $(\text{MgZn}_2)$ ; as well as  $(\text{CaZn}_{13})$ ,  $(\text{MgZn}_2)$  and  $\text{Mg}_2\text{Zn}_{11}$  compounds. The morphology along the diffusion zone in the solid-solid DC2 is completely different from that of the solid-solid DC1. The diffusion reaction starts from the two-phase terminal member:  $(\text{IM1}) + (\text{Mg})$ , as illustrated in Fig. 3(a). Then with the gradual change of the Mg concentration, from the left hand side to the right hand side of the diffusion couple, less Mg exists in the IM1 matrix in this direction. Afterwards, the matrix dramatically changed from IM1 to IM3 solid solution, the morphology also changes to isolated  $\text{MgZn}_2$  precipitates imbedded in the IM3 matrix. Then, the IM3 matrix changes to  $\text{CaZn}_{13}$ , which contains 6.4-15.5 at.% Mg and the same isolated  $\text{MgZn}_2$  precipitates. After that, the morphology of the reaction layer changes gradually, exhibiting another two-phase structure consisting of the same  $\text{CaZn}_{13}$  matrix, but with different Mg concentration (3.8-6.4 at.%), then the diffusion zone changes to the end member Zn.

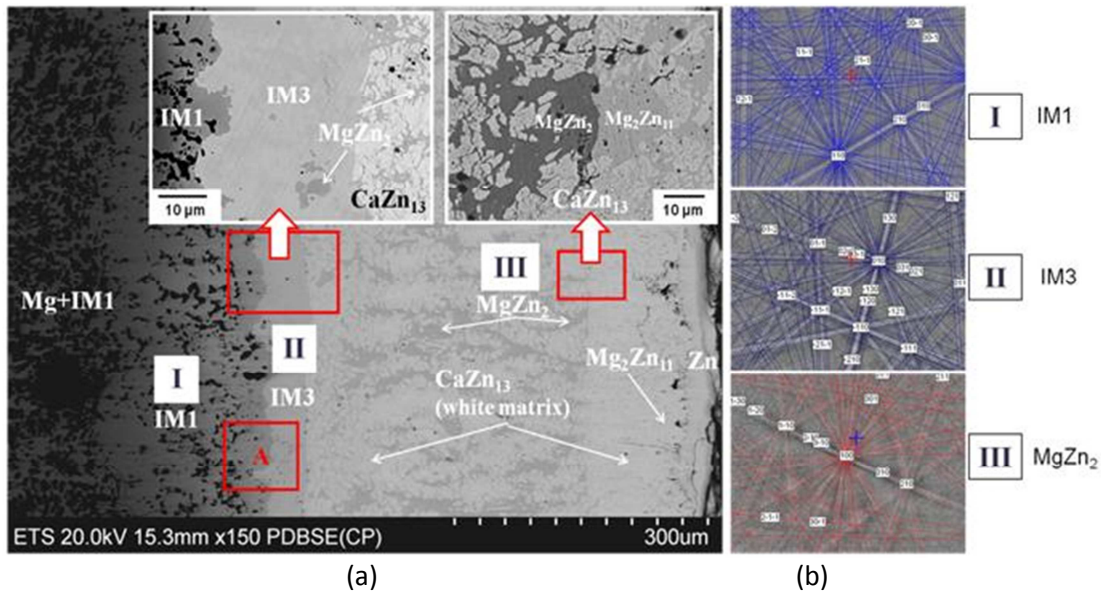


Fig. 3. (a) BSE images of the solid-solid DC2 annealed at 335°C for 4 weeks showing the formation of five intermetallic compounds; (b) indexed EBSD patterns of (I) IM1 and (II) IM3 ternary compounds and (III) MgZn<sub>2</sub> binary compound having extended solid solubility into ternary system.

The crystallographic orientation distribution and morphology of the IM1 and IM3 grains along the diffusion couple were analyzed using EBSD orientation mapping and pole figures. Although the direction of phase growth is parallel to the diffusion direction, the pole figure (Fig. 4) reveals that no clear preferred crystallographic orientation can be observed for both ternary compounds (marked as square A in Fig. 3(a)). Hence the direction of the diffusion does not cause the crystals to grow in a certain preferable orientation in the diffusion layers. The EBSD analysis was also carried out at the interface of the diffusion regions (Fig. 5) to study the misorientation of crystals within a grain and crystal orientation relations between the IM1 and IM3 compounds. Figs. 5 and 6 show the observation of very little cumulative misorientation, i.e. less than 1 degree, within each grain of IM1 or IM3 phase across the interface. It means that no significant distortion or rotation is happening along the grain at the interface. The crystals in the grain grow in the directions parallel to the direction of the initial nucleus orientation. The analysis of more than 50 pairs of the IM1 and IM3 grains orientation at the grain boundaries has shown no clear tendency in terms of their joint orientation. That means that the growth directions of the IM1 and IM3 phases are completely independent from each other.

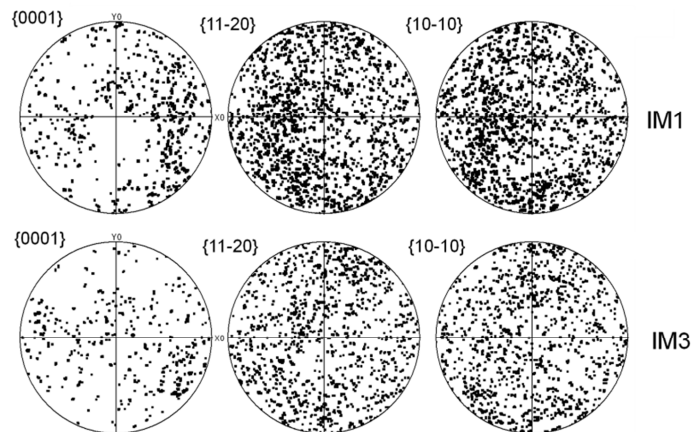


Fig. 4. Pole figures for IM1 and IM3 ternary compounds

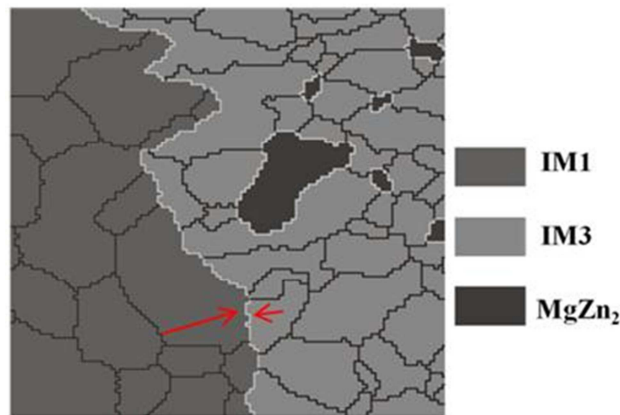


Fig. 5. EBSD phase mapping

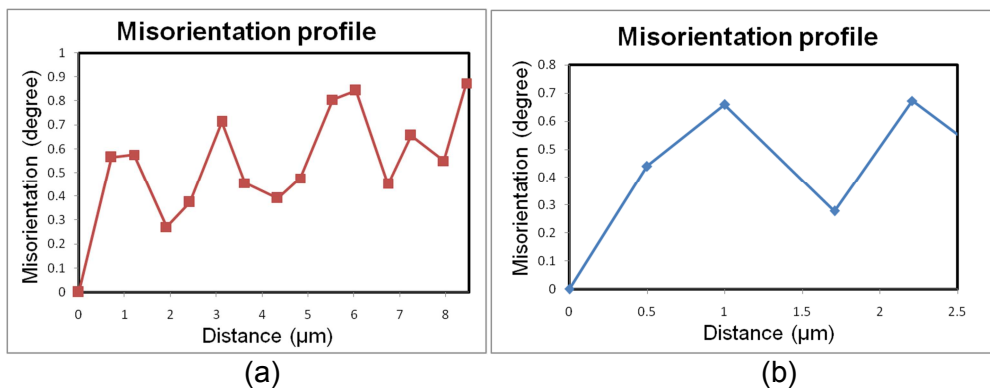


Fig. 6. Misorientation profile along a grain of (a) IM1, (b) IM3 at the interface

### Summary

The morphological and crystallographic characterizations of the Ca-Mg-Zn intermetallics were investigated through diffusion couples at 335°C. Phase relations, solubility limits and crystallographic information were determined for the binary and ternary compounds using SEM, EPMA, and EBSD. Depending on the different terminal compositions of the diffusion couples, the morphology may evolve as tooth-like structures, a matrix phase with either isolated or dendritic precipitates. Electron back-scattered diffraction analysis was carried out to investigate the crystal orientation of the IM1 and IM3 ternary compounds and the crystal orientation relations at the interface of the diffusion regions. Crystallographic analysis along the diffusion couple does not show clear preferred orientation and no trend with certain misorientation was found between IM1 and IM3 compounds at their interface.

### Acknowledgments

Financial support from General Motors of Canada Ltd. and NSERC through the CRD grant program is gratefully acknowledged. The authors would also like to thank Pierre Hovington from Hydro-Quebec research center for his help in sample preparation for EBSD analysis.

### References

- [1] A.A. Luo, Recent Magnesium Alloys Development for Elevated Temperature Application, *International Materials Review*, Vol.49, No.1, 2004, pp. 13-30.
- [2] M. Aljarrah, M. Medraj, X. Wang, E. Essadiqi, G. Dénès and A. Muntasar, Experimental Investigation of the Mg-Al-Ca System, *Journal of Alloys and Compounds*, Vol. 438, No. 1-2, 2007, pp. 131-141.
- [3] F. Nie and B.C. Muddle, Precipitation Hardening of Mg-Ca (-Zn) Alloys, *Scripta Materialia*, Vol.37, No.34, 1997, pp. 1475-1481.

- [4] B. Zberg, P.J. Uggowitzer, and J.F. Löffler, MgZnCa Glasses Without Clinically Observable Hydrogen Evolution for Biodegradable Implants, *Nature Materials*, Vol. 8, 2009, pp. 887-891.
- [5] B. Zberg, E.R. Arataa, P.J. Uggowitzer, and J.F. Löffler, Tensile Properties of Glassy MgZnCa Wires and Reliability Analysis Using Weibull Statistics, *Acta Materialia*, Vol. 57, No. 11, 2009, pp. 3223-3231.
- [6] E. Ma and J. Xu, Biodegradable Alloys: The Glass Window of Opportunities, *Nature Materials*, Vol. 8, 2009, pp. 855-857.
- [7] R. Paris, Ternary Alloys, Publications Scientifiques et Techniques du Ministère de L'Air, *Ministère de L'Air*, No.45, 1934, pp. 1-86.
- [8] J.B. Clark, The Solid Constitution in the Mg-rich Region of the Mg-Ca-Zn Phase Diagram, *Trans. AIME*, Vol. 221, 1961, pp. 644-645.
- [9] J.B. Clark, *Joint Committee on Powder Diffraction Standards (JCPDS) Card 12-0266*, 1961.
- [10] T.V. Larinova, W.W. Park, and B.S. You, A Ternary Phase Observed in Rapid Solidified Mg-Ca-Zn alloys, *Scripta Materialia*, Vol. 45, 2001, pp. 7-12.
- [11] P.M. Jardim, G. Solorzano, and J.B.V. Sande, Precipitate Crystal Structure Determination in Melt Spun Mg-1.5wt%Ca-6wt%Zn Alloy, *Mircoscopy and Microanalysis*, Vol. 8, 2002, pp. 487-496.
- [12] K. Oh-ishi, R. Watanabe, C.L. Mendisa, and K. Hono, Age Hardening Response of Mg-0.3 at.% Ca alloys with different Zn contents, *Materials Science and Engineering: A*, Vol. 526, No. 1-2, 2009, pp. 177-184.
- [13] Y.N. Zhang, D. Kevorkov, J. Li, E. Essadiqi, M. Medraj, Determination of the Solubility Range and Crystal Structure of the Mg-rich Ternary Compound in the Ca-Mg-Zn System, *Intermetallics*, Vol. 18, No. 12, 2010, pp. 2402-2411.
- [14] J.B. Clark, *Joint Committee on Powder Diffraction Standards (JCPDS) Card 12-0569*, 1961.
- [15] J. B. Clark, Conventions for Plotting the Diffusion Paths in Multiphase Ternary Diffusion Couples on the Isothermal Section of a Ternary Phase Diagram, *Transactions of the Metallurgical Society of AIME*, Vol. 227, 1963, pp. 1250-1251.
- [16] A.A. Kodentsov, G.F. Bastin, and F.J.J. van Loo, The Diffusion Couple Technique in Phase Diagram Determination, *Journal of Alloys and Compounds*, Vol. 320, No. 2, 2001, pp. 207-217.
- [17] J.C. Zhao, A Combinatorial Approach for Efficient Mapping of Phase Diagram and Properties, *Journal of Materials Research*, Vol. 16, No. 6, 2001, pp. 1565-1578.
- [18] J.C. Zhao, M. R. Jackson, and L.A. Peluso, Determination of the Nb-Cr-Si Phase Diagram Using Diffusion Multiples, *Acta Materialia*, Vol. 51, No. 20, 2003, pp. 6395-6405.
- [19] S. Wasiur-Rahman and M. Medraj, Critical assessment and thermodynamic modeling of the binary Mg-Zn, Ca-Zn and ternary Mg-Ca-Zn systems, *Intermetallics*, Vol. 17, No. 10, 2009, pp. 847-864.
- [20] P. Villars, K. Cenzual, Pearson's Crystal Data - Crystal Structure Database for Inorganic Compounds (on CD-ROM), Release 2009/2010, ASM International, Materials Park, Ohio, USA.